Entropy and fractal analysis of brain-related neurophysiological signals in Alzheimer's and Parkinson's disease

IOP Publishing J. Neural Eng. 20 (2023) 051001 https://doi.org/10.1088/1741-2552/acf8fa

Journal of Neural Engineering

OPEN ACCESS

RECEIVED
16 December 2022

REVISED
27 July 2023

ACCEPTED FOR PUBLICATION
12 September 2023

PUBLISHED
25 September 2023

TOPICAL REVIEW

Entropy and fractal analysis of brain-related neurophysiological signals in Alzheimer's and Parkinson's disease

Alberto Averna[1,3,4], **Stefania Coelli**[2,4], **Rosanna Ferrara**[2,3,5], **Sergio Cerutti**[2], **Alberto Priori**[3] and **Anna Maria Bianchi**[2,*]

[1] Department of Neurology, Bern University Hospital, University of Bern, Bern, Switzerland
[2] Department of Electronics, Information and Bioengineering, Politecnico di Milano, Piazza Leonardo da Vinci 32, 20133 Milan, Italy
[3] CRC 'Aldo Ravelli' per le Neurotecnologie e le Terapie Neurologiche Sperimentali, Dipartimento di Scienze della Salute, Università degli Studi di Milano, via Antonio di Rudinì 8, 20122 Milano, Italy
[4] These authors contributed equally.
[5] Currently working at Dipartimento di Ingegneria dell'Informazione ed Elettrica e Matematica applicata/DIEM, Università degli studi di Salerno.
[*] Author to whom any correspondence should be addressed.

E-mail: annamaria.bianchi@polimi.it

Keywords: nonlinearity, Parkinson's disease, Alzheimer's disease, EEG, LFP, fractals, entropy

Abstract

Brain-related neuronal recordings, such as local field potential, electroencephalogram and magnetoencephalogram, offer the opportunity to study the complexity of the human brain at different spatial and temporal scales. The complex properties of neuronal signals are intrinsically related to the concept of 'scale-free' behavior and irregular dynamic, which cannot be fully described through standard linear methods, but can be measured by nonlinear indexes. A remarkable application of these analysis methods on electrophysiological recordings is the deep comprehension of the pathophysiology of neurodegenerative diseases, that has been shown to be associated to changes in brain activity complexity. In particular, a decrease of global complexity has been associated to Alzheimer's disease, while a local increase of brain signals complexity characterizes Parkinson's disease. Despite the recent proliferation of studies using fractal and entropy-based analysis, the application of these techniques is still far from clinical practice, due to the lack of an agreement about their correct estimation and a conclusive and shared interpretation. Along with the aim of helping towards the realization of a multidisciplinary audience to approach nonlinear methods based on the concepts of fractality and irregularity, this survey describes the implementation and proper employment of the mostly known and applied indexes in the context of Alzheimer's and Parkinson's diseases.

1. Introduction

Cognitive and motor functions of the human brain are the result of complex dynamics generated and maintained at different spatial and temporal scales [1], characterized by nonlinear properties. Nonlinear behaviors can be approached in terms of fractality, which is associated with a scale-invariant (i.e. 'scale-free') and 'self-similar' behavior; and in terms of unpredictability, also called 'entropy' [2, 3].

Indeed, theoretical (ideal) fractals are objects showing scale-invariant behavior [4], that, in the spatial domain, are 'self-similar' geometric items with features on an infinite number of scales and their hallmark is a power-law scaling. In a real scenario, as for natural (statistical) fractals, scale-invariance holds only for a limited range of scales related to a particular scaling range [5]. Such scale-invariant behavior can also occur in the temporal domain. In fact, these temporal fractals exhibit fractally correlated events over different time scales. In time-series, scale-invariant behavior is a representation of a hierarchy of both temporal and spatial scales that may cover the wide range between coarse-scale long-term and short-term fine-scale fluctuations [6]. The self-similarity property of time-series can be evaluated by analyzing the

presence of a power law relationship between frequency (f) and the size of the process variation in a log–log scale plot. Specifically, the $1/f\hat{}\beta$ characteristic means that the power of the process is inversely proportional to its frequency, where β is known as the power or spectral exponent [7]. This concept is usually employed synonymously with long-range temporal correlation (LRTC) and as such represents a correlated phenomenon. LRTC can be measured in several ways. Popular methods include the Hurst exponent (HE), detrended fluctuation analysis (DFA) and multifractal analysis (e.g. MF-DFA) [8, 9]. Of note, multifractal time series are fractal time series that require more than one scaling exponent to be effectively described [10] and may reveal higher order correlations.

On the other hand, the complexity of a system can be represented by the unpredictability of the generated time series, which can be easily quantified evaluating its 'Entropy' [11, 12]. Several measures exist to estimate the entropy or irregularity of a process, with the common interpretation that an irregular and complex process is less predictable than a regular one, leading to a higher entropy value [13]. In the time domain, popular entropy indexes, such as the approximate entropy (ApEn) [14] and the sample entropy (SampEn) [15], have been introduced specifically for the study of biological time series and have also been widely used to study brain behavior.

In neuroscience, fractal and entropy indexes have been used to quantify the dynamical activity of the brain in different conscious states [16] and mental disorders [17]. In particular, alterations of some fractal and entropic properties have been suggested to underlie neurodegenerative disorders and may have important clinical implications for diagnosis and prediction of patients' outcomes [18, 19]. Particular attention has been paid to Alzheimer's (AD) and Parkinson's (PD) diseases as they are two of the most prevalent neurodegenerative diseases in the world [20]. Although AD and PD may exhibit numerous shared clinical and pathological features, they are characterized by distinct etiological mechanisms and involvement of different brain regions which can be analyzed through electrophysiological recordings and can result in altered complexity of brain signals [21]. Interestingly, in the literature, fractal and entropy measures have been used to characterize the complexity of brain activities in these neurodegenerative diseases leading to results that are consistent with known structural brain changes due to the pathologies.

Nonetheless, nonlinear methods for time series analysis in the neurological domain remain scarcely implemented and poorly understood due to their nontrivial physiological and clinical interpretation. Moreover, attention should be paid to the identification of the most appropriate techniques and the correct parameters to be applied for different types of data. Thus, the characterization of each type of signal should guide the choice of the processing method and of the parameters to be used.

The present survey aims at helping the reader to understand the basic implementation and application of most diffused nonlinear methods for evaluating the dynamic characteristics of electrophysiological signals. At the same time, the ability of such methods to evaluate changes in complexity induced by AD and PD is reviewed.

For this survey, we performed a search in PubMed and Web of Science databases using as keywords 'Entropy', 'fractal analysis' for the analysis methods, 'Alzheimer's disease' 'AD' and 'Parkinson's disease' for the pathology and electroencephalogram 'EEG', local field potential 'LFP' and magnetoencephalogram 'MEG' for the brain signals. We further considered works between 2005 and 2022, published in peer-reviewed journals. To focalize the review, we selected fractal and entropic parameters that were mainly represented in the bibliographic outputs, applied in a univariate fashion (i.e. papers dealing with complexity of functional connectivity measures were excluded). Within the selected papers, relevant references matching our criteria were also included. We summarize the reviewed papers in table 1, which is complemented by table 2 reporting a brief description of the neurophysiological signals considered and their main characteristics. The selected papers identified the most used indices for the non-linear analysis of the neurological signals, while theoretical and methodological papers were also included.

The selected methods are here described in detail and grouped in two sections: (a) $1/f$ power-law exponent, HE, Higuchi fractal dimension (HFD) and DFA grouped in the section named Fractal analysis and (b) Shannon entropy (H), ApEn, SampEn, permutation entropy (PeEn) and multiscale entropy (MSE) in the section named Entropy analysis.

The most important results, together with their proposed clinical interpretation devoted to the comprehension of the pathophysiology of these diseases are finally summarized in table 3.

2. Fractal analysis

Fractals are complex systems which are characterized by fractional dimensions, a concept that goes beyond the classical geometry, meaning that a complex signal could be represented by non-integer dimension: for example more than a line (characterized by

Table 1. Summary of the reference dealing with the application of fractal and entropy analysis in Alzheimer's and Parkinson's diseases literature.

Alzheimer's disease				Parkinson's disease			
References	Signal	Fractal	Entropy	References	Signal	Fractal	Entropy
Abásolo *et al* [22]	EEG		ApEn				
Stam *et al* [23]	EEG	DFA		Lim *et al* [24]	Spike trains		ApEn
Escudero *et al* [25]	EEG		MSE (SampEn)	Hohlefeld *et al* [26]	LFP	DFA	
Park *et al* [27]	EEG		MSE (SampEn)	Chung *et al* [28]	EEG		MSE (SampEn)
Hornero *et al* [29, 30]	MEG		ApEn	Herrojo Ruiz *et al* [31]	LFP	DFA	
Abásolo *et al* [32]	EEG	DFA	ApEn	Huang *et al* [33]	LFP	β exp (IRASA)	
Montez *et al* [34]	MEG	DFA		Hohlefeld *et al* [35]	LFP	DFA	
Gomez *et al* [36]	MEG		ApEn, SampEn	Alam *et al* [37]	Spike trains		ApEn
Mizuno *et al* [38]	EEG		MSE (SampEn)	West *et al* [39]	LFP	DFA	
Poza *et al* [40]	MEG		SampEn, others	Yuvaraj and Murugappan [41]	EEG	HFD	
Yang *et al* [42]	EEG		MSE	Syrkin-Nikolau *et al* [43]	LFP		SampEn
Zorick and Mandelkern [44]	EEG	MF-DFA		Liu *et al* [45]	EEG		SampEn
Labate *et al* [46]	EEG		MSE (SampEn, PeEn)	Yi *et al* [47]	EEG		PeEn
Vysata *et al* [48]	EEG	β exp		Martin *et al* [49]	LFP	β exp	
Deng *et al* [50]	EEG		PeEn	Mostile *et al* [51]	EEG	β exp	
Smiths *et al* [52]	EEG	HFD		Belova *et al* [53]	LFP	β exp	
Coronel *et al* [54]	EEG		H, MSE (SampEn)	Pappalettera *et al* [55]	EEG		ApEn
Tylová *et al* [56]			PeEn				
Nimmy John *et al* [57]	EEG	HE					
Nobukawa *et al* [58]	EEG	HFD					
Amezquita *et al* [59]	EEG	HFD, HE					
Echegoyen *et al* [60]	MEG		PeEn				
Zorick *et al* [9]	EEG	MF-DFA					
Seker *et al* [61]	EEG		PeEn				
Ando *et al* [8]	EEG	MF-DFA	MSE				

a dimension = 1) and less than an area (characterized by dimension = 2) and can be described by a dimension value between 1 and 2 (fractional dimension) [62]. One of the main properties of fractal systems, and then of fractal time series, are scale invariance and self-similarity [7].

Fractal time series are characterized by a 'fractal dimension' (FD) which statistically represents how much a pattern changes as a function of the observation scale. The FD can be computed according to several definitions [63], but this procedure can be easily described through the 'box counting' algorithm by starting to count the number of 'boxes' of a given size necessary to cover the analyzed time series, as represented in figures 1(a) and (b). The procedure is repeated many times changing the box size, *l*. The FD, which can take non-integer values, is defined as the negative of the slope in the bi-logarithmic plot of the number of boxes in function of their size *l*, (see figures 1(c) and (d) for details). In general, the more complex the signal, the higher the FD.

Although methods for measuring the fractal behavior of a time series may differ in their operational domain and produce measures of self-similarity in different ways, they share some properties; among them the already mentioned power-law behavior which can be quantified and described through different analysis and parameters. For this reason, in this section we grouped together the $1/f$ power-law exponent (β), HE, DFA and the HFD techniques under the single category 'Fractal analysis'. Before describing the equations linking these analyses, an important step is to identify the class to which the analyzed time series belongs. Generally, as basic references, one should consider two classes of fractal signals, fractional Gaussian noises, fGn, and fractional Brownian motions, fBm. Ideally, a long memory process signal should be categorized as either stationary (fGn) or non-stationary (fBm) according to this definition [64]. Moreover, only fBm signals are characterized by a fractal structure having self-similar behavior, while fGn, signals have a

Table 2. Summary of different type of biological signals employed and relative characteristics (origin, spatial resolution and frequency content), usual acquisition devices and pre-processing steps are also reported.

				Application in the reviewed papers	
Type of signal	Type, origin and spatial resolution (scales level)	Frequency content (Hz)	Acquisition and pre-processing	Disorder	Non-linear indexes
Local field potential (LFP)	*Electric potential* of small population of cortical neurons and cerebral structure. (*Meso-scale* level $\sim$1 mm)	0.5–500	Implanted electrodes for clinical purposes, such as the recording lead of the DBS neurostimulator in PD. Pre-processing steps are needed to remove noises and typical artifacts, such as line noise, heart-related artifacts, subject's movements, and stimulation artifacts.	PD	ApEn SampEn, DFA β
Electroencephalography (EEG)	*Electric potential* of large populations of neurons at the scalp. (*Macro-scale* level $>$ 1 cm)	0.5–50	Scalp EEG routinely performed in clinical setting and for research protocols with up to 256 electrodes on the scalp. Pre-processing steps are needed to remove noises and typical artifacts, such as ocular movements, muscular activity, line noise, heart-related artifacts, and subject's movements. Signal analysis is then performed in the time and frequency domain both at the sensors and at the source level.	PD/AD	H ApEn SampEn PE MSE DFA β MF-DFA
Magnetoencepalography (MEG)	*Magnetic fields* generated by the activity of large populations of neurons. (*Macro-scale* level $\sim$1 cm)	0.5–200	Mainly performed for research studies, MEG systems use a variable number of magnetometers or/and gradiometers (more than 300 is possible). Pre-processing steps are needed to remove noises and typical artifacts, such as ocular movements, muscular activity, line noise, heart-related artifacts, and subject's movements. Signal analysis is mainly performed at in the sources space.	AD	ApEn SampEn PE DFA

Table 3. Summary of main results and their clinical interpretation of Alzheimer's and Parkinson's- related nonlinear analysis literature.

	Main results	Clinical interpretation
	Alzheimer's disease	
Fractal	Overall EEG frontal-occipital decrease of power-law exponent. Greater variance of β-values respect to controls [48]. Larger values of Hurst exponent in temporal lobes with respect to subjects with no cognitive decline. High variation of values in the right hemisphere of patients [57]. Aberrant autocorrelation structure of temporo-parietal alpha oscillation and medial prefrontal theta in early-stage AD [9, 34].	Lower β-values were associated to changes of neuronal connectivity compromised by presence of brain atrophy [48]. Larger values of Hurst exponent associated to difficulty in memorizing while variation suggested damages with consequent difficulty in motor skills [57]. Both DFA exponent and MF-DFA correlated to severity of disease [9, 34]. Combined use of DFA and spectral analysis in AD patients improved diagnostic [110].
Entropy	Exclusively applied to EEG and MEG signals. The most recurring result reports a decreased entropy with respect to age-matched controls.	Lower entropy in AD patients is interpreted as the result of a loss of structural complexity and functional connectivity [25].
	Parkinson's disease	
Fractal	Flatter PSD-slope in fronto-temporal sites with respect to healthy controls [51]. Steeper PSD-slope under the effect of general anesthesia [33]. Presence of LRTC in the high-frequency gamma range increased by Levodopa and positive correlation between cortex and basal ganglia across multiple time scales [26, 35]. Emergence of LRTC with DBS On [31].	Flatter slope linked to higher irregularity, while steeper to decrease of complexity [51]. Changes in PSD-slope considered highly related to the balance excitation/inhibition [33]. LRTC is a potential biomarker of pathological processes in PD [26, 35]. Positive correlation between DFA-PS exponent and motor impairments [3].
Entropy	Local higher entropy in brain activity with respect to controls [28, 37] and the modulation of the LFP and neuronal signal irregularity in relation to PD's symptoms.	Higher entropy of the basal ganglia activity associated to a more error-prone and less efficient motor information transfer. Increase of beta entropy during FOG events interpreted as a compensatory attempt to correct the abnormal activity [43].

self-similar appearance only when their amplitude is rescaled by the HE [5].

fBm, fGn, β and HE are then linked by the relations [5, 65, 66]:

$$\beta_{\mathrm{fBm}} = 1 + 2\mathrm{HE}_{\mathrm{fBm}}$$

$$\beta_{\mathrm{fGn}} = 2\mathrm{HE}_{\mathrm{fGn}} - 1$$

while the fluctuation exponent α, resulting from the DFA method (see section detrended fluctuation analysis (DFA)), can be related to HE according to the formulas [5, 65, 66]:

$$\alpha_{\mathrm{fBm}} = 1 + \mathrm{HE}_{\mathrm{fBm}}$$

from which we obtain:

$$\beta_{\mathrm{fBm}} = 2\alpha_{\mathrm{fBm}} - 1$$

$$\alpha_{\mathrm{fGn}} = (\beta_{\mathrm{fGn}} + 1)/2.$$

It is worth noting that, despite fBm and fGn are intrinsically characterized by the same HE exponent, fBms represent non-stationary signals with time dependent variance, while fGns are stationary processes with constant mean and constant variance over time.

Distinguishing between fGn and fBm series is possible, in principle, from the evaluation of their β, as fGn corresponds to β exponents ranging from 1 to $+1$ (α [0:1]), and fBm to β exponents from $+1$ to $+3$ (α [1:2]) [64, 65].

2.1. Power-law exponent

Fractals can be measured using a power-law relationship. In mathematical terms, a power-law is a form of scale-invariance where one quantity varies proportionally to a power of the other. Application of power-law behavior in time-series usually comes with a log–log plot, where the axes represent the power spectrum density (PSD) function of the signal and its frequency. The PSD of a signal describes the linear distribution of the spectral power over the frequency components (figure 2) and the focus of the analysis is usually on the

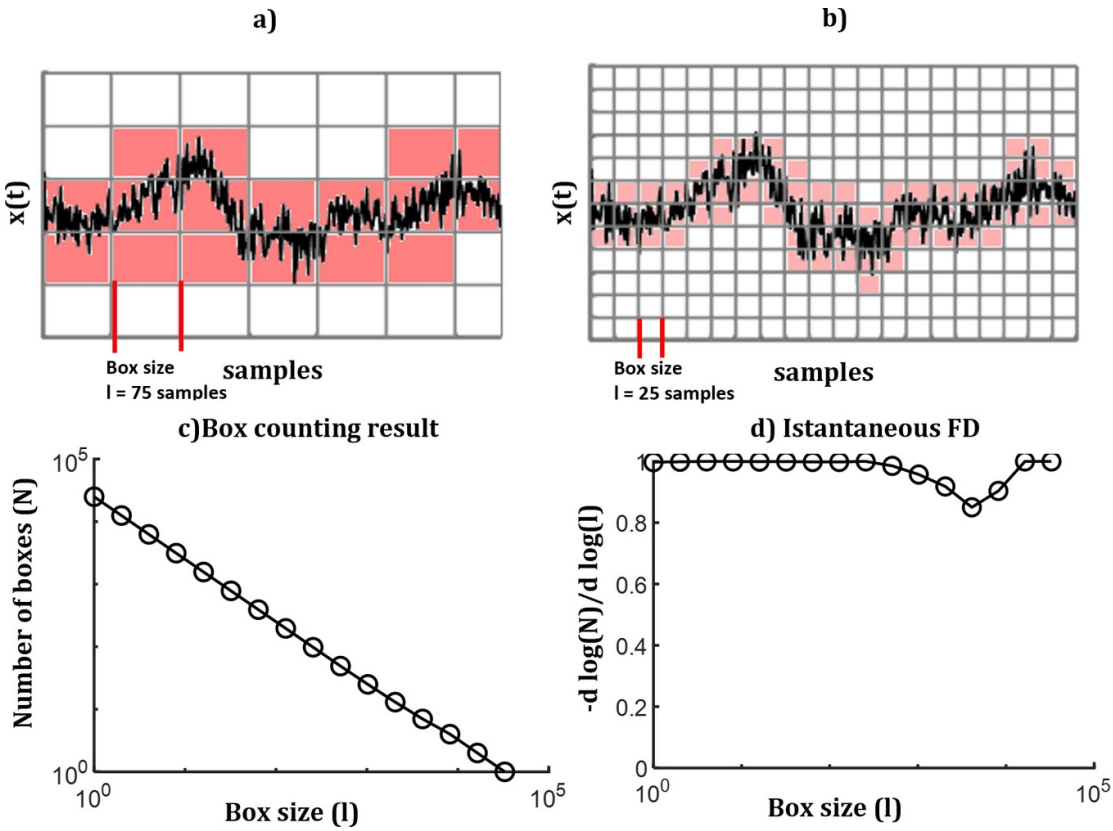

Figure 1. Application of the box counting procedure to a portion of a local field potential (LFP) signal. The signal, or curve, is divided in elements (boxes) of different size l and the number of elements needed to cover the curve is counted for each l. (a) $l = 75$ sample and (b) $l = 25$ samples. (c) To derive Fractal dimension (FD) of the curve, from the box counting algorithm (box-counting dimension), the number of boxes N is plotted against the size l in log–log scale and the negative of the slope of the obtained curve is taken. (d) Semi-log plot of the local slope of the curve in (b) as a function of the size. If the slope is constant in a range of different sizes, this slope is a good estimation of the FD of the curve. The LFP signal in (a) was acquired from a Parkinsonian patient.

oscillatory components figure 2(b) which, to be non-linearly evaluated, need the application of complex methods, such as higher order spectral analysis [67, 68]. The power-law decay of the spectrum as a function of frequency is also called '1/f noise' and characterizes the non-oscillatory and fractal-behavior of signals [69, 70].

When considering the PSD in log–log coordinates (figure 2(c)), obtained through estimation approaches (i.e. Welch's method [49, 51, 53, 71] or the multi-taper spectrogram method [33]), it is possible to extract information about the 1/f behavior [71]. In details, the log–log plot shows how the log(PSD) linearly changes with respect to log(frequencies); then, an operation of linear regression on the spectral power is performed to estimate a straight line that represents the statistical 'self-similarity' (which is a typical property of statistical fractals) of the signal. The slope of the line is used to estimate the scaling exponent β, also called power-law exponent. The fractal component tends to be analytically characterized by $\frac{1}{f^{\beta}}$, where β is a constant that defines the kind of dynamic behavior of the signal [5]. For example, $\beta = 0$ characterizes white noise-like systems, which are uncorrelated time series and have a power spectrum that is independent of the frequency. Time series with $\beta = 1$, are called flicker or 1/f noise systems, which are moderately correlated, while Brownian noise-like systems are represented by $\beta = 2$, which are strongly correlated. Nevertheless, it is important to point out that it is impractical to use the spectral exponent β as an indirect means of quantifying the fractal dimension FD (as this latter is only defined for fBm type signals [5]) although these methods exist in literature [72, 73], due to the several steps of approximation required to fit the spectral decomposition of a time series. Critical aspects in the estimation of the power-law exponent are: (i) the frequency ranges on which to estimate the linear slope; (ii) the frequency resolution (and then the signal length) needed for a robust linear slope estimation, also taking into consideration that at the lower frequencies in the log scale, the spectral points available for the linear regression are less than at the higher frequencies, and then the estimation has a higher uncertainty.

Moreover, it is important to remark that neurophysiological signals are highly characterized by oscillatory components. To prevent that the estimation

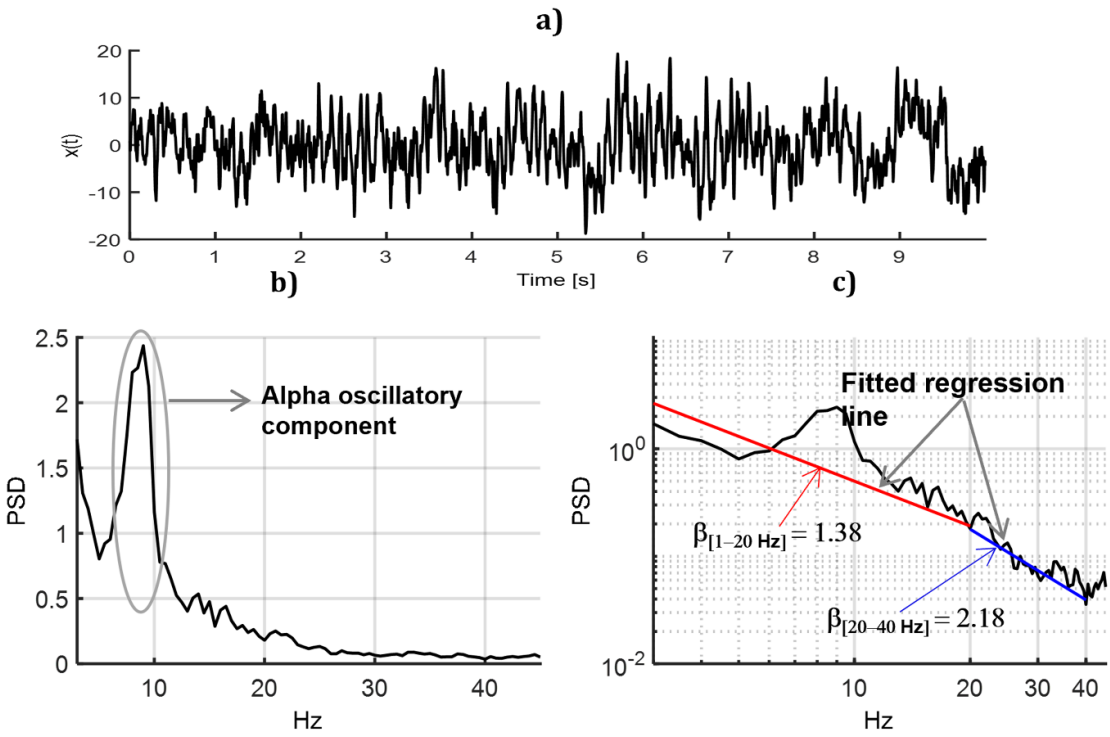

Figure 2. (a) 10 s of an EEG signal from a healthy volunteer acquired at rest with a sampling rate of 256 Hz. (b) Power spectral density (PSD) obtained with the Welch's method averaging 2 s windows. In linear scale, the oscillatory component associated to the alpha rhythm is clearly visible. (c) The same PSD is plotted in log–log scale to enhance the $1/f$ background component. Two regression lines are fitted and plotted considering two different frequency ranges (i.e. 1–20 Hz and 20–40 Hz) and the correspondent power-law exponents β are estimated.

of β might be compromised by the rhythmic oscillatory components, several methods have been proposed, in addition to the simpler peak suppression [74, 75]. The first one is the coarse graining spectral analysis [76]. It separates the harmonic and the scale-free components of the power spectrum using the self-similarity property of the fractal time series: indeed, in fractal time series the statistical distribution does not change when data are sampled at different frequencies, and this is not valid for harmonic time series. The method is based on modifying the sampling frequency of the time-series by a factor λ, in order to obtain the 'coarse grained series', and on computing the cross-power spectrum from this series and the original one ($S_{xx_\lambda}(f)$); if this tends to 0, the signal is simply periodic or oscillatory, while, if it follows a power-law distribution, the signal is fractal [71, 77]. Another technique is called irregular-resampling auto-spectral analysis (IRASA) and is based on resampling the original signals by a couple of factors (positive numbers and their reciprocals) and on computing the mean of the auto-power spectra of each pair of the resampled signals. As a result, the power associated to the rhythmic components are redistributed in the resulting spectrum, while the power of the component $1/f$, extracted taking the median of the mean auto-power spectra, remains independent from h factors [77]. An alternative approach, known as the 'fitting oscillations & one over f' (FOOOF) method, is designed to model periodic components of the spectrum [69]. The FOOOF method iteratively applies Gaussian fits to all the oscillatory components, resulting in a model of the periodic part. By subtracting this periodic model from the spectrum, a potentially pure aperiodic component, suitable for fitting β is obtained.

2.2. Hurst exponent (HE)

The HE measures the self-similarity and the correlation properties of the fractal time series, indicating the level of persistence (i.e. the property according to which the value of the variable at a certain time is closely related to the previous value) of the series [63, 78]. It can be used to evaluate the smoothness of a time series; indeed, it is related to the fractal dimension (FD). Such relationship is defined through:

$$\mathrm{FD} = 2 - \mathrm{HE}$$

with $0 \leqslant \mathrm{HE} \leqslant 1$ [79]. The fact that the exponent can assume only values within the range [0,1] implies that (i) for HE $= 0.5$ the series under analysis is completely random; (ii) for HE > 0.5 it shows low self-similarities (a persistent behavior) which corresponds to a smoother trend, (iii) HE $\leqslant 0.5$ indicates that the temporal series have a high self-similarity (an anti-persistent behavior), indicating a rougher graph [63, 78, 79]. In order to account for the different classes

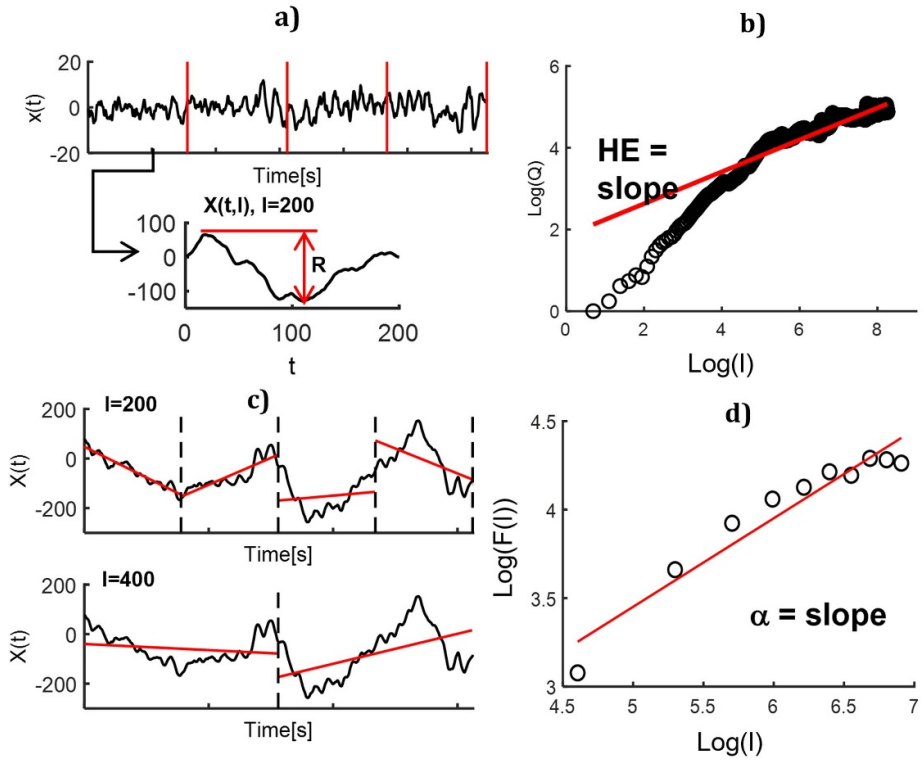

Figure 3. Schematic representation of the Hurst exponent (HE) and DFA estimation procedure applied to the same signal of figure 2. (a) Rescaled range method: the time series is divided into segments of l samples each from which the integrated series $X(t,l)$ is obtained. The range R is computed from $X(t,l)$ and divided by the segment standard deviation to obtain the rescaled range Q. (b) Log–log plot of Q in function of the segment size l. The slope of the fitting line is the estimated HE. (c) To perform the DFA the integrated series $X(t)$ is divided in non-overlapping segments of size l on which the data are fitted with a least-square line representing the trend. (d) Log–log representation of the size of the fluctuation $F(l)$ in function of the segment size. The α index is estimated as the slope of the regression line fitting the data in the double logarithmic plot. The represented signal is the same from figure 2.

of signals (i.e. fGn and fBm) an extend version of the HE was developed, by defining $0 < \mathrm{HE} < 1$ for fGn and $1 < \mathrm{HE} < 2$ for fBm [80]. The HE, like the entropy, provides a measure of the complexity of the signal: increase of the value of HE indicates less complexity and higher synchronization [81]. There are several algorithms that can be used to estimate HE parameter [63]. One of these is based on the *rescaled range* (figure 3(a)), which measures how the variability of the time series changes with the length of the period.

The HE is estimated dividing the signal into segments of length l and computing on each segment its range R

$$R(l) = \max_t X(t,l) - \min_t X(t,l)$$

with $1 \leqslant t \leqslant l$ while $X(t,l)$ are the integrated series defined as the cumulative sum

$$X(t,l) = \sum_{k=1}^{t} [x(k) - \bar{x}],$$

where $\bar{x}$ is the mean of the considered segment.

To obtain the rescaled range $Q(l)$, $R(l)$ is divided by the standard deviation SD of the original signal within the segment. $Q(l)$ is computed for each segment of length l and then averaged to obtain $\bar{Q}(l)$. This procedure is repeated for all the possible segment of size l. Thus, it is possible to estimate the HE as

$$\mathrm{HE} = \frac{\log(\bar{Q}(l))}{\log(l)}.$$

That is the slope of $\log(\bar{Q}(l))$ in function of $\log(l)$ as in figure 3(b), obtained by an operation of linear regression [65]:

$$\bar{Q} \propto l^{\mathrm{HE}}.$$

2.3. Detrended fluctuation analysis (DFA)

DFA was first proposed by Peng *et al* [82] in order to estimates long-range correlations in DNA sequences but it found applicability in many other contexts, such as measures of long-time weather records [83], hearth rate dynamics [84, 85] as well as sea clutter radar data [86]. A signal is said to exhibit long-range dependencies if non-zero correlation exists between its samples even when separated by long time intervals. Nowadays, it is a widely used method to estimate the extent of so-called 'long-range temporal correlations (LRTCs)' present in a signal [87, 88]. It is aimed at assessing the level of self-similarity in a time

series by representing the relationship between the variability of the signal and the length of the intervals over which such variability is computed. The DFA algorithm can be implemented by following three steps (as schematized in figure 3):

(i) A temporal series $x(t)$ of length L ($t \in L$) is first integrated as follows:

$$X(t) = \sum_{k=1}^{t} (x(k) - \bar{x})$$

where $X(t)$ is the cumulative sum and $\bar{x}$ is the mean of the time series $x(t)$.

(ii) $X(t)$ is then divided into k non-overlapping intervals of length l and within each interval, a least-squares straight line is fitted to the data, representing the trend in that window (figure 3(c)), that is denoted by X_j^{Th}. Thus, for a given interval length l, the size of fluctuation for the integrated and detrended series is calculated as:

$$F(l) = \sqrt{\frac{1}{L}\sum_{j=1}^{l}\left(X_j - X_j^{Th}\right)^2}.$$

(iii) This computation is finally repeated over all time scales (window sizes l) to obtain the relationship between $F(l)$ and the window size (figure 3(d)). Typically, $F(l)$ increases with window size. The statistical self-similarity of the signal is represented by a straight line in the log–log graph of $F(l)$ versus l and the fractal scaling exponent α from the slope of the line. Indicating the self-similarity with $F(l) \propto l^{\alpha}$, the fluctuation exponent α characterizes signals that can exhibit either correlated (in the form of LRTCs with $\alpha > 0.5$) or uncorrelated ($\alpha < 0.5$) processes.

The multifractal DFA (MF-DFA) method is a generalized method of DFA that allows a characterization of multifractal (higher order) scaling behavior of time series [89]. While DFA uses only the second order moment (i.e. $q = 2$), MF-DFA is based on the scaling of the qth order moments, thus providing the following qth order fluctuation function:

$$F_q(l) = \left\{\frac{1}{L}\sum_{j=1}^{l}[F(l)]^{q/2}\right\}^{1/q}.$$

The scaling exponent $\alpha(q)$, which for $q = 2$ is identical to HE, is determined by analyzing log–log plots $F_q(l)$ versus l for each value of q. Thus, when long-term correlation occurs in the data, a behavior like $F_q(l) \propto l^{\alpha(q)}$ appears on $F_q(l)$ [89].

2.4. Higuchi fractal dimension (HFD)

The HFD of a time series, HFD, is a measure of irregularity and is calculated directly in the time domain [62]. For electrophysiological signals the HFD usually returns a value between 1 and 2 where, the higher the HFD value, the higher the signal complexity and, consequently, the lower its fractal properties. As reported in [62] if the power-law exponent $1 \leqslant \beta \leqslant 3$, then the fractal dimension FD $= (5-\beta)/2$, thus for $\beta \to 1$ then FD $\to 2$ which corresponds to uncorrelated white noise while for $\beta \to 3$ then FD $\to 1$ which corresponds to the highest level of self-similarity in the time series.

Multiple time series at a variety of different time scales are first generated by subsampling the signal repeatedly:

$$X_k^i; X(i), X(i+k), X(i+2k), \ldots \times X\left(i + \left[\frac{N-i}{k}\right]k\right) \qquad (i = 1, 2, \ldots, k).$$

Being X is the original signal, i the starting time, k the interval time and N the number data points, the algorithm then calculates the average length $L(k)$ of the curve across all the k intervals as:

$$L_i(k) = \frac{1}{k}\left(\sum_{j=1}^{\left[\frac{N-i}{k}\right]}(X(i+jk) - X(i+(j-1)k))\right) \times \left(\frac{N-1}{\left[\frac{N-i}{k}\right]k}\right)$$

where the term $\frac{N-1}{\left[\frac{N-i}{k}\right]k}$ is a normalization factor. If $L(k)$ follows a power law, then curve is fractal with dimension D:

$$L(k) \propto k^{-D}.$$

HFD is represented by the slope of the lined formed by the double logarithmic graph of $L(k)$ of each k.

3. Entropy-based analysis

The term entropy in information theory is commonly referred to the amount of 'uncertainty' in the information content of a system generating the process explained by a time series. Shannon [11] and Kolmogorov–Sinai [12] proposed different formulation of 'Entropy', to estimate the predictability of the analyzed signal.

In the biomedical field, these approaches are principally known for their large application and consensus for the study of the heart rate variability (HRV)

signal [63, 90], but they have also been applied in the study of brain functions and dysfunction [16, 17]. Besides the classical Shannon entropy (H), the most frequently used approaches are the ApEn, the SampEn, the PeEn, and the MSE.

The *Shannon entropy* [11] quantifies the amount of information carried by a time series $x(t)$ as a function of the probability of occurrence of each sample $p(x(t))$. Such a probability could be estimated from a large amount of signal values, ideally infinite ($N \to \infty$). The Shannon entropy (H) is then defined as the negative summation over the time sample t of such probability multiplied by its logarithmic value,

$$H = -\sum_{t} p(x(t)) \cdot \log(p(x(t))).$$

Since the biological systems, generating the process we are measuring, are dynamical systems, the carried information varies over time. To capture this property, the Kolmogorov–Sinai entropy was introduced to express a measure of 'entropy rate', that is the average rate at which a system produces information. For a random process $\{x(t)\}$ at a time t, it is defined as $H(x) = \lim_{t\to\infty} H(x_1, x_2, \ldots, x_t)$. This concept is derived from the *Conditional Entropy* defined as $CE(x) = \lim_{t\to\infty} H(x_t|x_{t-1}, x_{t-2}, \ldots)$, which measures the amount of predictability of future values in a time series given its past values, meaning that if the past information produced by a system can accurately explain its current state, the system is predictable (the $CE(x)$ is low), if not, it is said unpredictable (the $CE(x)$ is high) [63, 91].

3.1. Approximate entropy (ApEn)

The ApEn, introduced by Pincus [92], based on the concept of $CE(x)$, measures the regularity and patterns repeatability in time series, even if of finite length and noisy. Briefly, ApEn of a signal of N points is defined as the average of the negative natural logarithm of the conditional probability that two sequences (or templates) in the signal contain similar patterns of m and $m+1$ points, with a tolerance r. The parameter m is called embedding dimension. Operatively, five main steps are needed to compute the ApEn of a given time series of N time points $\{x(t)\,|1 \leqslant t \leqslant N|\}$, here described and represented in figure 4(a) for an exemplificative embedding dimension $m = 2$:

(1) A series of $N - m - 1$ templates of size m, $T_m(j) = \{x(j+k), with\, k = 0, \ldots, m-1\}$, is defined for $1 \leqslant j \leqslant N - m + 1$;
(2) The distance between two templates $T_m(j)$ and $T_m(i)$ is than taken as the maximum difference of their samples $d(T_m(j), T_m(i)) = \max_{0\leqslant k\leqslant m-1} |x(j+k) - x(i+k)|$; with $1 \leqslant i \leqslant N-m+1$
(3) We then call Z_j^m the number of $T_m(i)$ templates in the signal for which $d(T_m(j), T_m(i)) \leqslant r$, i.e. the number of patterns of m time points which are similar to the given template $T_m(j)$ with tolerance r. The regularity of the pattern in the time series is measured by the probability expressed as $C_j^m(r) = Z_j^m/(N-m+1)$ that any template $T_m(i)$ is similar to $T_m(j)$ with tolerance r. Tolerance is represented by the distance between horizontal solid lines in figure 4(a).
(4) Now it is possible to define the function $\Phi^m(r) = \sum_{j=1}^{N-m+1} \log C_j^m(r)/(N-m+1)$ as the average of the natural logarithms of the probabilities $C_j^m(r)$ over j;
(5) We than repeat step 1 to step 4 for $m+1$ and finally obtain the estimation of the statistics for finite time series of length N as $\mathrm{ApEn}(m, r, N) = \Phi^m(r) - \Phi^{m+1}(r)$.

It is evident that ApEn is dependent on the length N of the time series, meaning that for short recording duration the estimated value will be lower than for longer ones. Therefore, to be comparable among different conditions, N should be fixed.

3.2. Sample entropy (SampEn)

SampEn was conceived by Richman and Moorman [15] to evaluate the randomness of the HRV signals. With the same objective of the ApEn, SampEn has being developed to reduce the dependency from the recording duration affecting ApEn. Therefore, SampEn can provide reliable results also with shorter N in comparison to ApEn, but still a bias can be introduced if a very short length is considered. Moreover, by eliminating the self-matches, the computation of SampEn has a computational cost reduced by one-half with respect to ApEn [15].

Indeed, to calculate the SampEn, we define W as the number of templates pairs of size $m+1$ for which $d(T_{m+1}(j), T_{m+1}(i)) \leqslant r$, with $i \neq j$ and V the total number of matches between templates of size m, again with $i \neq j$ (i.e. excluding self-matching).

Their ratio (W/V), which represent the conditional probability, that the distance between two templates of size m is within a tolerance r and will remain within r at the next sample, is used in the final computation $\mathrm{SampEn} = -\log(W/V)$.

Both ApEn(m,r) and SampEn(m,r) were introduced to be applied on short and continuous time series with respect to previous entropy measures, but still, parameters m and r should be properly set and N also considered. In both cases, there is not a 'perfect' rule for the selection of parameters, m and r. In the field of HRV, Pincus suggested that for a reliable ApEn estimation m should be set to 2 and r in the range between 0.1 and 0.25 times the standard deviation of the data, and N larger than 10^m or, better, at least 30^m samples [14]. In line with these suggestions, also for the SampEn it was proposed

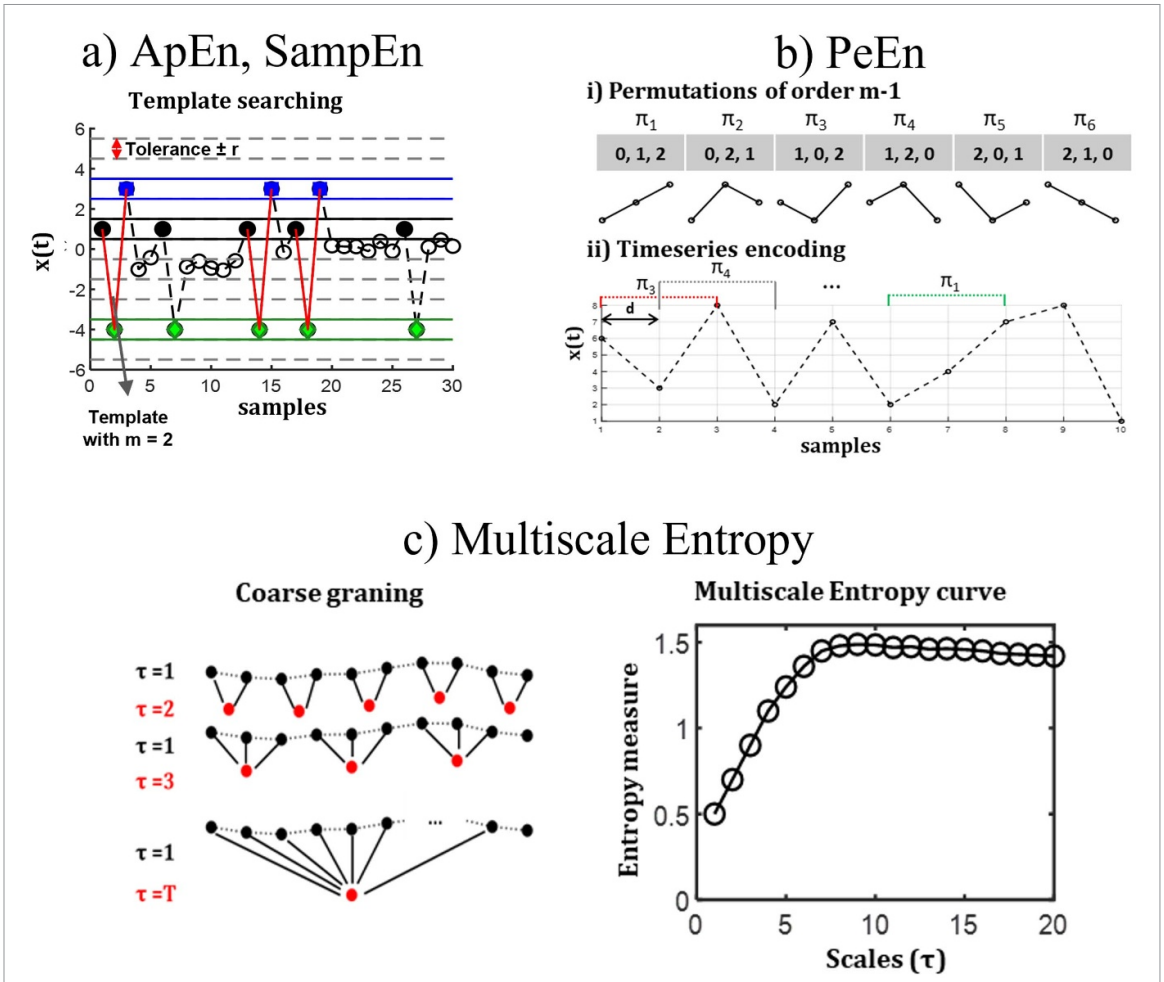

Figure 4. (a) For a given signal $x(t)$, the computation of both ApEn and SampEn is based on the probability of matching the template of $m + 1$ points (black–green–blue dots) if the template of m points (black-green dots) matched with a distance $d(T_m(j), T_m(i)) \leqslant r$. (b) Example of the encoding procedure for the calculation of the PeEn with $m = 3$ and $d = 1$. (i) Given the embedding dimension $m = 3$, the possible permutations (or amplitude rankings) π_k of order $m - 1$ are 6 and are represented by the rank values in sequences. (ii) The timeseries is divided in sequences of m samples, with a delay d. The amplitude value of each sample is replaced by its rank so that a series of permutations is encoded. Thus, a probability distribution of the permutations is obtained. (c) MSE calculation example. The entropy measure is computed at different temporal scales obtained with a coarse-graining procedure, i.e. averaging the values of τ samples at each scale from 2 to T, where T is the maximum value of scale factor. The value of the entropy index is plotted in function of the time scale and the MSE curve is obtained. All the images were built on signals constructed for representative purposes only as random signals with superimposed identifiable patterns (a) and (b) or simply random signals (c).

to set $m = 1$ or 2 and r in the range between 0.1 and 0.25 times the standard deviation of the data, but a much shorter signal length, still of at least 10^m samples, is considered sufficient as demonstrate in [15]. These parameter values are often taken as appropriate also for neurophysiological signals, but, as discussed in section 4, such an approach could be a limitation.

Both ApEn and SampEn describe the signal regularity at a fixed time scale and ignore its variability structure that could arise at different time scales (i.e. different frequency ranges). In the context of biomedical signals, M/EEG in particular, the time scale, or frequency range, at which the analysis is performed has great importance, since it may reflect specific underlying processes [93].

3.3. Permutation entropy (PeEn)

A noteworthy alternative to the aforementioned entropy indexes, is the PeEn [94, 95], based on the concept of Shannon Entropy. Introduced to deal with the non-stationarity of the signals, PeEn works by applying an embedding procedure to the analyzed signal, with embedding dimension m, and time-lag d. An example of this embedding procedure is represented in figure 4(b) for an embedding dimension $m = 3$ and a lag $d = 1$.

Briefly, the time series is cut into segments of dimension m delayed by d samples. The samples of the segments are arranged in increasing order and converted in ordinal patterns of order $m - 1$. Thus, instead of creating templates based on the amplitude values, patterns are created considering the

rank of each sample (i.e. if the amplitude pattern is {6, 3, 7}, this is converted to a sequence of ranks {1, 0, 2} for a pattern of order $m = 3$), making it robust to noise. For an embedding dimension m, the possible order of patterns, or *permutations* π, will be $m!$. Considering the resulting symbolic series in which each symbol corresponds to a permutation, PeEn is obtained estimating the Shannon Entropy of the relative frequencies for each possible permutation of order $m > 2$

$$\mathrm{PeEn} = -\sum_{i=1}^{m!} p(\pi_i) \cdot \log(p(\pi_i)).$$

Higher the PeEn value, higher the signal irregularity [94]. The algorithm to obtain the PeEn is very fast and works with short time series. As the ApEn and the SampEn, also the PeEn has been employed in the MSE framework [46].

3.4. Multiscale entropy (MSE)

The MSE was proposed as an extension of the SampEn algorithm to capture the information of a system at different time scales [96]. The computation of the MSE is built on two steps: (i) the construction of a set of coarse-grained time series, and (ii) the estimation of a measure of entropy (e.g. ApEn, SampEn, etc) at each time scale. Given a time series of N points $x(t)$, the coarse-grained time series $\{y_n(\tau)\}$, determined by the scale factor τ, are constructed replacing τ samples by their average (figure 4(c)), thus it corresponds to the application of a low pass filter followed by sub-sampling.

The calculated entropy measure is then plotted as a function of the coarse-graining scale factor, τ. This approach allows the assessment of the dynamic evolution of the signal structure and can be related to its frequency content. In fact, as shown by Courtiol *et al* [93], the down sampling operation of the coarse-graining framework, has the effect of removing the fast oscillations so that, at increasing time scales, we measure the entropy of the slower oscillations. To obtain a concise complexity index, the area under the MSE curve is often computed [63].

4. Confounding factors

All the methods described share the drawback of being dependent on factors and parameters that are not always directly under the control of the experimenter. In this section, the principal confounding factors influencing the reliability of the fractal and entropy analysis are introduced.

The common factors that induce misinterpretation of fractal and entropy analysis derive from the typical compromise that must be reached between a sufficient large length of the recording, that should be enough to reach statistically significant results, and the possible presence of non-stationarities, due to the characteristic weak stationarity (or a 'wide-sense' stationarity) of brain signals. As reported by several studies the use of series of 2^9 or 2^{10} data points is considered as an acceptable compromise to satisfy the requirements of nonlinear methods (stationarity and sufficient amount of data points) and, at the same time to correctly perform experiments involving brain signals (e.g. in order to optimize the spectral analyses for neuronal signals) [5, 65, 97]. Therefore, it is evident that fractal and entropy measures cannot be applied when the experimental paradigm comprises the analysis of short, discontinuous, and transient responses, such as evoked or event-related potential.

In *Fractal Analysis*, the specific 'class' of the time series (i.e. determined by their distinction into fGn and fBm) is another factor that may influence the result interpretation. Several authors [5, 64, 65, 98, 99] claim that the scaling exponent can be properly assessed using a method relevant for the identified class. Despite a proper preprocessing of the 'raw' data prior to analysis might minimize the effects of non-stationarities on the scaling properties of the data [100], it is certainly not trivial establishing the correct class of a neurophysiological signal. Moreover, even if PSD and DFA algorithm seem very reliable to estimate the fractal exponent of a fGn, on the other hand they are negatively biased and produce high variability of results when applied to a fBm [65]. The preliminary classification of series as fGn or fBm is indeed a crucial step for correctly approaching fractal analysis. Furthermore, brain-related signals are typically 'noisy', and exhibit different types of non-stationarities (such as the presence of discontinuities as well as spikes that are independent on the fluctuation of the signal), which might be removed before running fractal analysis [100]. The different nature of the signals can also affect the value, and interpretation of the estimated feature, as shown in [101] regarding the difference between the power-spectral exponent computed on EEG and MEG signals.

The selection of the fitting range boundaries for analyzing the power-law exponent also requires careful consideration, as it may introduce biases in the estimation, potentially leading to incorrect interpretation of the outcomes [102]. In general, there is not a universal fitting range that suits all types of PSDs. For example, if the fitting range is too narrow, it may not fully cover the entire span of aperiodic activity, resulting in an inaccurate estimation of β. Conversely, if the fitting range is too wide, it might include oscillatory components or other non-$1/f$-like fluctuations, introducing biases in the estimation. Therefore, it is recommended to carefully examine the PSDs of interest and choose a fitting range that effectively capture the $1/f$ characteristic.

A prominent confounding factor of Entropy-based measures is their parametric nature [63]. While the Shannon Entropy needs the definition of the probability distribution of the data, that cannot be

known in advance, Approximate, Sample and PeEn need the definition of the embedding dimension parameter m and, in the first two cases, the tolerance r, time-lag d, in the latter case. To the best of our knowledge, no studies provide rules for tuning them on neural signals, therefore guidelines proposed for HRV analysis are often applied. This lack of knowledge represents a real barrier to the correct application, meaningful interpretation and repeatability of entropy indexes extraction from brain related signals in different contexts and studies.

The introduction of the MSE has improved the application of entropy measures to non-stationary neurophysiological signals by allowing a more detailed observation of the signal complexity at different time scales. Nevertheless, the analysis of MSE stability and the few guidelines for its application to real brain signals proposed by Kuntzelman *et al* [103] and by Courtiol *et al* [93] should be deepened and properly considered.

4.1. Assessing the statistical significance of the estimation

Due to the natural variability of neurophysiological signals an appropriate statistical test with the aim of establishing the reliability of estimation methods is needed. One method to test the accuracy and precision of the nonlinear analysis is given by the use of surrogate data [63, 104]. Several surrogate generation algorithms, each of them addressing a particular null hypothesis, have been proposed in literature. These include for example random shuffled surrogates, phase-randomized surrogates (based on the Fourier transform) [104] or amplitude adjusted Fourier transform surrogates, but many other additional algorithms have also been proposed (see [105] for a recent review). The idea behind such an approach is to determine if the value of the nonlinear measures obtained on real data is not obtained by chance. To this aim these algorithms consider a large number of surrogate time series that are derived from real signals with different time domain behavior but same linear properties (such as mean, variance and autocorrelation function) [105]. Thus, such generation of a distribution of data, composed by copies of the original signals with the same statistical properties, but disrupted nonlinear properties, allows to test for significance the outcomes of both fractal and entropic algorithms ensuring their validity.

5. Application of nonlinear methods in neurodegenerative diseases

Understanding brain complexity is crucial for unraveling the mechanisms underlying neurological disorders such as Alzheimer's and Parkinson's disease. Although AD and PD are related to different functional domains (i.e. cognitive and motor, respectively), both diseases generally lead to neurodegenerative dementia, which includes a range of symptoms such as cognitive decline, that have been related to changes in the structural and functional complexity of the brain. Brain-related neurophysiological signals from patients with neurodegenerative diseases are typically evaluated analyzing their oscillatory components in the frequency domain [106–109]. However, the complexity of brain signals is thought to reflect the degree of abnormality as well as the pathological features of the aforementioned diseases (table 1), and therefore *Fractal* or *Entropy* methods have been widely used to characterize them. In this section, we reviewed works using *Fractal* or *Entropy* analysis for the characterization of Alzheimer's and Parkinson's diseases.

5.1. Fractal analysis application

5.1.1. Power-law exponent

The possible role of the β exponent as an EEG-based biomarker to discriminate PD patients from healthy controls (HCs) was tested by Mostile *et al* [51]. The authors extracted β in a broad frequency range, without controlling for the presence of high frequency noise. They found significantly lower β values at the left fronto-temporal sites in PD patients when compared to HC. Such a result was interpreted as the presence of a higher level of local fractality and self-similar behavior in PD patients than in HCs. It is worth noting that the power-law exponent has been shown to be modulated by aging, therefore is not clear whether the observed changes are related to a physiological alteration due to aging or to pathology. Further studies, comparing elderly subjects with and without Parkinson's disease, could help to understand the real effects of the disease on the power-law component.

The modulation of the power-law component by pharmacological intervention in PD patients, such as during the administration of propofol, has also been studied. Huang *et al* found [33] a steeper PSD slope (calculated in the range [2–80] Hz and extracted with the IRASA method from LFP recordings in the subthalamic nucleus (STN)) during the loss of responsiveness after propofol injection compared to the awake state [33]. This variation was interpreted by the authors as a decrease of the excitation/inhibition (E/I) balance causing a steeper power-law in the STN activity. However, it is not clear whether these results reflect the symptoms of the pathology: in fact, even if the study was conducted on a group of PD patients, it must be taken into account that they were treated during the recordings; therefore, Huang *et al* [33] hypothesized that similar results could be obtained by conducting similar analysis in the anesthetized healthy brain [33]. The

claim that the β slope is related to the E/I ratio in the STN of PD patients was also supported in [53], since β was found to be modulated by movements in a population of 22 PD patients undergoing DBS implantation.

Vysata *et al* [48] compared the power exponent values in resting EEGs of AD patients and HCs. The authors found lower β in frontal and temporal EEG sites and a greater variance in patients, similarly to the results reported by Mostile for PD subjects. Such results were interpreted as reflecting the presence of a neuroanatomical connectivity impairment related to the brain atrophy. Based on previous work, the authors hypothesized that there is a link between the physiological mechanism that dissipates energy in the brain and its connectivity. Therefore, the presence of brain atrophy, which occurs in AD, would affect the dissipation of energy, affecting the $1/f$ component [48].

5.1.2. Hurst exponent (HE)

Few studies used the HE to analyze EEG in patients affected by the neurodegenerative disorders. Nimmy John *et al* [57] compared the EEG between Alzheimer's patients and normal subjects at rest and during cognitive tasks. Larger HE values were found in the temporal lobes of patients with mild cognitive impairment (MCI)-AD compared with controls, which means that the decrease in randomness correlates with the difficulty in memorizing visual and verbal information. Moreover, a large variation of HE in the right hemisphere of the patients' brains was also found. This change suggests a damage reflected in the reduction of non-verbal thinking and difficulty in controlling motor skills. All these aspects were in line with results obtained from behavioral tests, such as The Mini Mental Status Exam (MMSE), the Rey Auditory Verbal Learning Test and Addenbrooke's Cognitive Examinations used to determine the cognitive impairment, memory problems and the level of progression of the disease, respectively.

EEG signals were analyzed by Amezquita-Sanchez *et al* [59] combining the nonlinear HE with the integrated multiple signal classification and empirical wavelet transform to distinguish AD patients from MCI patients. The HEs estimated for AD patients resulted lower than those for MCI; this outcome was attributed to the presence of less self-similarities, that means greater complexity, for Alzheimer's patients with respect to the MCI patients. The cited studies suggest that patients with AD and MCI have a reduced complexity compared to healthy subjects, but at the same time patients with MCI show greater self-similarity with respect to AD patients.

Our survey did not find any relevant literature reporting HE analysis on Parkinson's disease.

5.1.3. Detrended fluctuation analysis (DFA)

A relatively small number of studies have investigated the role of LRTCs measured by DFA in neurodegenerative diseases, providing new insights into their pathophysiology and suggesting novel markers for disease monitoring.

The combined use of DFA and spectral analysis on EEG signals of AD patients was shown to improve the diagnostic accuracy thus complementing the classification based on spectral analysis [110]. Stam *et al* in 2005 used the DFA algorithm to determine changes in the synchronization level in EEG different frequency bands of Alzheimer's patients. They found that spontaneous changes of synchronization of EEG signals were lower in AD in upper alpha and beta bands compared to non-AD patients and that DFA exponents were correlated to the severity of the disease [23]. In [34], Montez *et al* measured brain activity with whole-scalp magnetoencephalography (MEG) in patients with early-stage AD and in age-matched control subjects. They used DFA to characterize the autocorrelation structure of amplitude fluctuations in neuronal oscillations on long time scales (1–25 s), discovering an aberrant autocorrelation structure of temporo-parietal alpha oscillation and of medial prefrontal theta activity, which may prove this index a useful biomarker of early-stage AD [34]. Multifractality (MF-DFA) has been also employed to predict the degree of cognitive impairment in AD. Zorick and Mandelkern, demonstrated that human EEG signals may be modeled as an underlying multifractal process [44] and that MF-DFA on EEG is a very promising method to accurately estimate the severity of disease in terms of MMSE score, as it was both sensitive and specific for clinical staging of both mild AD and MCI [9].

DFA has also been used in Parkinson's disease to assess for LRTCs in patients implanted with DBS electrodes in the STNs. Hohlefeld *et al* [26] showed the presence of prominent LRTC in the very high-frequency gamma range (>200 Hz) of STN, especially when treated with the dopamine-precursor drug Levodopa. In [35] the same authors reported a positive correlation between neural dynamics of the most dominant rhythms in the cortex (alpha, 8–13 Hz) and basal ganglia (beta, 10–20 Hz) across multiple time scales and suggested a further model of cortical–subcortical interaction [35]. Another study proved the clinical relevance of LRTC in a single patient with idiopathic PD and right-handed tremor [31]. The patient was asked to play piano pieces with and without active DBS, demonstrating the onset of long-range correlations of isochronous inter-onset interval (i.e. the time between the onsets of two successive piano notes) only when DBS was active, together with an overall motor improvement in the tremor-affected hand. In addition, another study on a group of PD patients undergoing DBS surgery found

the presence of LRTC in the dynamics of the bilateral STN, both ON and OFF levodopa administration using an adaptation of DFA to study synchronization [39], called DFA-PS initially proposed in [111]. Also, in this study, authors found a positive correlation between the DFA-PS exponent and motor impairments in patients during OFF condition.

5.1.4. Higuchi fractal dimension (HFD)

Not many studies have measured the complexity of brain activity through the HFD in the context of Parkinson's and ADs. In one study [41], Yuvaray and Murugappan have used HFD and other nonlinear features to build two different classifiers aimed at recognizing the emotional states of both left- and right-side affected PD patients. They found that patients mainly suffering from right-hemisphere dysfunction were more impaired in emotional communication compared to left-hemisphere pathology suggesting an asymmetric neuronal degeneration involved into the impairment of emotional communication of PD.

In Alzheimer disease, HFD has been demonstrated to be a sensitive indicator of neuronal changes in comparison to healthy aging. In particular, Smiths *et al* [52] found that HFD is reduced in AD and this reduction was associated to the decreased cognitive capacity of the patients, thus highlighting the ability of this measure to quantify the loss of neural efficiency and reduced cortical communication in AD. In another study, Nobukawa *et al* investigated the temporal-scale-specific fractal properties of EEG signals recorded from both AD and healthy subjects. Consistently with the hypothesis that that EEG signals in AD exhibit less complexity [112], the authors found a reduced fractality at both slow and fast temporal scales for the AD group which correlated with the cognitive decline [58].

5.2. Entropy analysis application

The 'Entropy Hypothesis' proposed in [113, 114] for the basal ganglia pathology suggests that an increased irregularity in the LFP signals and complex, nonlinear temporal pattern in firing activity characterize the dynamics of the basal ganglia in patients affected by Parkinson's disease. On the other hand, different entropy and complexity measures have been employed to analyze the background activity of AD and PD patients' EEG or MEG at the scalp level to test the hypothesis of a loss of complexity due to neurodegeneration. In the following sections, we report results obtained using each of the described entropy indexes to analyze brain related activity in PD and AD patients.

5.2.1. Approximate entropy (ApEn)

In human subjects, spike trains acquired during DBS surgery were analyzed using ApEn to identify nonlinear characteristics of firing activity in the internal Globus Pallidus (GPi) and in the STN [24, 37]. Lim *et al* [24], applied the ApEn(2, 0.15) to interspike-intervals (ISI) sequences of surgical data acquired in GPi, external Globus Pallidus (GPe) and STN of 20 PD patients receiving DBS and compared the ApEn extracted from the data to the ApEn computed on shuffled ISIs series. Their results suggested the presence of nonlinear temporal organization of the firing, but the study lacked a control group. Using the same approach, Alam *et al* [37] reproduced those results in the GPi of 29 PD patients and provided a comparison to a control group composed of 13 patients affected by Dystonia receiving DBS under the same conditions. Their work confirmed an abnormal irregularity or entropy in the GPi neuronal activity in Parkinsonism. At the scalp level, the recent EEG study of Pappalettera [55] reported a not area-specific higher ApEn(2, 0.2), thus a higher complexity, in a group of PD patients with respect to age- and gender-matched controls.

ApEn has also been used to study the loss of complexity in AD affected brain. In their preliminary study, Abásolo *et al* [22] found a reduced ApEn ($m = 1$, $r = 0.2$) at the parietal region in AD patients respect to age matched controls and, simultaneously, a slower EEG activity was also observed. On MEG data, complementary studies employing SampEn, ApEn, Lempel-Ziv complexity and HFD, further confirmed the complexity reduction in a large cohort of AD and control subjects [29, 36, 40].

5.2.2. Sample entropy (SampEn)

In line with the 'Entropy hypothesis', Syrkin-Nikolau [43] related the increase of signal irregularity to the freezing of gait (FOG) in 14 freely moving PD patients by estimating the SampEn($m = 2$, $r = 0.2$) of band-pass filtered LFP signals recorded with DBS electrodes. The study suggested that higher entropy in beta filtered LFP signals indicates a less efficient and more error prone transfer of information in the basal ganglia, but alternative hypothesis cannot be excluded yet [43]. The SampEn of the EEG signal at rest was also shown to perform well in the discrimination of PD subjects in a classification approach, supporting the usefulness of the entropy approach to further study parkinsonism [45].

Concerning the AD, SampEn is largely applied in a multi scale approach as reported in section 5.2.4.

5.2.3. Permutation entropy (PeEn)

In contrast with results obtained with SampEn and ApEn indexes, PeEn computed in EEG resting state recordings of 18 PD patients was found reduced in the beta and gamma frequency bands, with respect to matched controls [47]. The authors interpreted their findings as a generalized reduction of brain complexity due to central nervous system impairment and suggested that such a result can also be associated to the presence of dementia in elderly-patients affected by Parkinson.

The reduction of complexity in AD was confirmed in [50] by computing the PeEn on EEG and exploring the effect of the used embedding dimension and time-lag. Recently, this result was confirmed and used to discriminate AD patients from healthy condition [61]. A novel approach for the computation of the PeEn was proposed in [56], studying, at the same time, the influence of the sampling frequency on the measure.

5.2.4. Multi scale entropy

Up to now only one relevant study applied MSE analysis to PD brain activity, while numerous studies applied this approach to EEG and MEG signals acquired on AD patients. Indeed, Chung *et al* [28] analyzed the sleep EEG data of 9 PD patients and 11 controls with the MSE approach and identified a higher complexity in the Parkinson group during non-REM sleep at higher time scales, in line with previously cited works employing entropy measures at the single scale.

On the same dataset analyzed in their earlier studies, Abásolo and colleagues applied the MSE approach based on the SampEn ($m = 1$, $r = 0.25$) and confirmed the previous findings supporting the conclusion that the brain activity of AD patients is less complex than in control subjects [25, 32]. More recently these results were confirmed in larger datasets [38, 54] and in MEG studies [29, 30, 36, 40]. Both Mizuno and Coronel applied MSE to resting state EEG signals and beyond the comparison with a control group, they tried to correlate the complexity measure with the severity score of the disease. In particular, Mizuno found that the complexity at higher time scales correlates with a measure of cognitive impairment [38], while Coronel obtained a good model to predict the severity score using MSE, Shannon Entropy and other complexity indexes [54]. Abnormal EEG complexity across short- and long-time scales was also reported in [42] where the consistency of the MSE was tested on different signal epochs and parameters ($m = 2$, $r = 0.15$) were optimized across 108 AD patients. MSE was found to particularly correlate with severity of cognitive and neuropsychiatric symptoms. Recently, the combination of MSE and MF-DFA was found to improve the accuracy of AD classifiers based on each if these metrics alone [8]. Moreover, the possibility to use entropy measures for predicting and characterizing the transition from MCI condition to AD has been foreseen by Park using MSE [27] and Labate [46] applying SampEn, Lempel-Ziv complexity and PeEn in a multiscale and multivariate approach.

Despite the highly concordant results, the pathophysiological implications are not completely clear yet. Taken together, these studies suggest that the loss of complexity in the EEG and MEG signal may reflect an actual loss of cortical functional organization and a less complex brain structure which result in a reduction of information processing [25, 40], particularly at lower temporal scales (higher frequency). It should be noticed, in fact, that Mizuno *et al* [38] observed an increased complexity in AD patients at larger temporal scales (lower frequency), probably reflecting long-range abnormal synchrony in the brain [17]. Therefore, as pointed out by the recent work of Echegoyen [60] applying PeEn on MEG data in three groups of subjects (i.e. Alzheimer patients, MCI and controls), there is not a trivial interpretation of the results, which are indeed heterogeneous at different frequency ranges and cortical regions.

6. Conclusions and perspectives

In the last two decades we have witnessed a growing interest in the use of *Fractal* and *Entropy* indexes for a better quantification and characterization of neurophysiological signals and for brain function monitoring in degenerative pathologies such as Alzheimer's (AD) and Parkinson's (PD) diseases. This reflects the need for tools that can complement the information provided by the current clinical standards and to provide better insight into pathologies that affect an ever-increasing number of people every day.

Nonlinear features can complement the information provided by linear indexes and are thus extremely valuable for a more complete characterization of these pathologies. On the other hand, their correct application to neurophysiological signals and their physiopathological interpretation remains controversial in several regards. The reasons could be mainly found in the intrinsic characteristics of the signals and in the difficulty to meet the required hypothesis for the correct application of the estimation procedures. As a matter of fact, many physical and biological signals, and in particular EEG, MEG and LFP are noisy, heterogeneous, and exhibit different types of non-stationarities, which can affect their long-term correlation and regularity properties. Moreover, all these indexes are based on different assumptions and hypothesis and have different properties leading to potentially controversial interpretations. A methodological effort is thus still required aimed at improving the reliability of these methods by defining strategies for the correct calculation and interpretation and for application to different biological time series.

The literature reviewed provides evidence that both fractal and entropy measures are sensitive to the change of functional and structural complexity in AD, resulting in a higher signal regularity (table 3). Indeed, several works have tried to exploit different non-linear indexes, including fractal and entropy measure, to discriminate AD patients from HCs and to classify the severity of the disease [8, 9, 40, 59]. The

systematic review by Tzimourta *et al* is recommended to interested readers [115].

Furthermore, the reviewed studies describe the subthalamic signals of PD patients as highly irregular, with a higher level of complexity if compared to control conditions, but results are less conclusive with respect to the AD research. Future studies are needed to assess the signal requirements (e.g. stationarity, length, noise level) and to identify the necessary parameters for the correct estimation of nonlinear indices. This step is necessary for the potential use of fractality and entropy measures as reliable biomarkers of neurodegenerative diseases.

Data availability statement

No new data were created or analysed in this study.

ORCID iDs

Alberto Averna https://orcid.org/0000-0001-9738-1281
Stefania Coelli https://orcid.org/0000-0003-4104-4790
Sergio Cerutti https://orcid.org/0000-0002-9607-8755
Alberto Priori https://orcid.org/0000-0002-1549-3851
Anna Maria Bianchi https://orcid.org/0000-0002-8290-7460

References

[1] Varela F, Lachaux J P, Rodriguez E and Martinerie J 2001 The brainweb: phase synchronization and large-scale integration *Nat. Rev. Neurosci.* **2** 229–39
[2] Goldberger A L 2006 Giles F. Filley lecture. Complex systems *Proc. Am. Thorac. Soc.* **3** 467–71
[3] West B J and Zweifel P F 1992 Fractal physiology and chaos in medicine *Phys. Today* **45** 68–70
[4] Mandelbrot B B 1977 *Fractal: Form Chance and Dimension* (W. H. Freeman and Co. Ltd)
[5] Eke A, Herman P, Kocsis L and Kozak L R 2002 Fractal characterization of complexity in temporal physiological signals *Physiol. Meas.* **23** R1
[6] Werner G 2010 Fractals in the nervous system: conceptual implications for theoretical neuroscience *Front. Physiol.* **1** 1787
[7] Mandelbrot B 1967 How long is the coast of Britain? Statistical self-similarity and fractional dimension *Science* **156** 636–8
[8] Ando M, Nobukawa S, Kikuchi M and Takahashi T 2021 Identification of electroencephalogram signals in Alzheimer's disease by multifractal and multiscale entropy analysis *Front. Neurosci.* **15** 1–11
[9] Zorick T, Landers J, Leuchter A and Mandelkern M A 2020 EEG multifractal analysis correlates with cognitive testing scores and clinical staging in mild cognitive impairment *J. Clin. Neurosci.* **76** 195–200
[10] Kantelhardt J W 2015 Fractal and multifractal time series *Encyclopedia of Complexity and Systems Science* (Springer) pp 1–37
[11] Shannon C E 1949 Communication theory of secrecy systems (https://doi.org/10.1002/j.1538-7305.1949.tb00928.x)
[12] Eckmann J P and Ruelle D 1985 Ergodic theory of chaos and strange attractors *Rev. Mod. Phys.* **57** 617–56
[13] Sun J, Wang B, Niu Y, Tan Y, Fan C, Zhang N, Xue J, Wei J and Xiang J 2020 Complexity analysis of EEG, MEG, and fMRI in mild cognitive impairment and Alzheimer's disease: a review *Entropy* **22** 239
[14] Pincus S M and Goldberger A L 1994 Physiological time-series analysis: what does regularity quantify? *Am. J. Physiol. Heart Circ. Physiol.* **266** H1643–56
[15] Richman J S and Moorman J R 2000 Physiological time-series analysis using approximate and sample entropy *Am. J. Physiol. Heart Circ. Physiol.* **278** 2039–49
[16] Keshmiri S 2020 Entropy and the brain: an overview *Entropy* **22** 917
[17] Takahashi T 2013 Complexity of spontaneous brain activity in mental disorders *Prog. Neuro-Psychopharmacol. Biol. Psychiatry* **45** 258–66
[18] Thamrin C, Stern G and Frey U 2010 Fractals for physicians *Paediatr. Respir. Rev.* **11** 123–31
[19] di Ieva A, Esteban F J, Grizzi F, Klonowski W and Martín-Landrove M 2015 Fractals in the neurosciences, part II *Neurosci* **21** 30–43
[20] Feigin V L *et al* 2019 Global, regional, and national burden of neurological disorders, 1990–2016: a systematic analysis for the Global Burden of Disease Study 2016 *Lancet Neurol.* **18** 459–80
[21] Keller S M, Reyneke C, Gschwandtner U and Fuhr P 2022 Information contained in EEG allows characterization of cognitive decline in neurodegenerative disorders *Clin. EEG Neurosci.* **54** 391–8
[22] Abásolo D, Hornero R, Espino P, Poza J, Sánchez C I and De La Rosa R 2005 Analysis of regularity in the EEG background activity of Alzheimer's disease patients with approximate entropy *Clin. Neurophysiol.* **116** 1826–34
[23] Stam C J, Montez T, Jones B F, Rombouts S A R B, van der Made Y, Pijnenburg Y A L and Scheltens P 2005 Disturbed fluctuations of resting state EEG synchronization in Alzheimer's disease *Clin. Neurophysiol.* **116** 708–15
[24] Lim J, Sanghera M K, Darbin O, Stewart R M, Jankovic J and Simpson R 2010 Nonlinear temporal organization of neuronal discharge in the basal ganglia of Parkinson's disease patients *Exp. Neurol.* **224** 542–4
[25] Escudero J, Abásolo D, Hornero R, Espino P and López M 2006 Analysis of electroencephalograms in Alzheimer's disease patients with multiscale entropy *Physiol. Meas.* **27** 1091–106
[26] Hohlefeld F U, Huebl J, Huchzermeyer C, Schneider G-H, Schönecker T, Kühn A A, Curio G and Nikulin V V 2012 Long-range temporal correlations in the subthalamic nucleus of patients with Parkinson's disease *Eur. J. Neurosci.* **36** 2812–21
[27] Park J-H, Kim S, Kim C-H, Cichocki A and Kim K 2007 Multiscale entropy analysis of EEG from patients under different pathological conditions *Fractals* **15** 399–404
[28] Chung C C, Kang J H, Yuan R Y, Wu D, Chen C C, Chi N F, Chen P C and Hu C J 2013 Multiscale entropy analysis of electroencephalography during sleep in patients with Parkinson disease *Clin. EEG Neurosci.* **44** 221–6
[29] Hornero R, Abásolo D, Escudero J and Gómez C 2009 Nonlinear analysis of electroencephalogram and magnetoencephalogram recordings in patients with Alzheimer's disease *Phil. Trans. R. Soc.* A **367** 317–36
[30] Hornero R, Escudero J, Fernández A, Poza J and Gómez C 2008 Spectral and nonlinear analyses of MEG background activity in patients with Alzheimer's disease *IEEE Trans. Biomed. Eng.* **55** 1658–65
[31] Herrojo Ruiz M, Hong S B, Hennig H, Altenmüller E and Kühn A A 2014 Long-range correlation properties in timing of skilled piano performance: the influence of auditory feedback and deep brain stimulation *Front. Psychol.* **5** 1030
[32] Abásolo D, Escudero J, Hornero R, Gómez C and Espino P 2008 Approximate entropy and auto mutual information

analysis of the electroencephalogram in Alzheimer's disease patients *Med. Biol. Eng. Comput.* **46** 1019–28
[33] Huang Y *et al* 2020 Dynamic changes in rhythmic and arrhythmic neural signatures in the subthalamic nucleus induced by anaesthesia and tracheal intubation *Br. J. Anaesth.* **125** 67–76
[34] Montez T *et al* 2009 Altered temporal correlations in parietal alpha and prefrontal theta oscillations in early-stage Alzheimer disease *Proc. Natl Acad. Sci. USA* **106** 1614–9
[35] Hohlefeld F U, Ehlen F, Tiedt H O, Krugel L K, Horn A, Kühn A A, Curio G, Klostermann F and Nikulin V V 2015 Correlation between cortical and subcortical neural dynamics on multiple time scales in Parkinson's disease *Neuroscience* **298** 145–60
[36] Gómez C and Hornero R 2010 Entropy and complexity analyses in Alzheimer's disease: an MEG study *Open Biomed. Eng. J.* **4** 223
[37] Alam M *et al* 2016 Globus pallidus internus neuronal activity: a comparative study of linear and non-linear features in patients with dystonia or Parkinson's disease *J. Neural Transm.* **123** 231–40
[38] Mizuno T, Takahashi T, Cho R Y, Kikuchi M, Murata T, Takahashi K and Wada Y 2010 Assessment of EEG dynamical complexity in Alzheimer's disease using multiscale entropy *Clin. Neurophysiol.* **121** 1438–46
[39] West T, Farmer S, Berthouze L, Jha A, Beudel M, Foltynie T, Limousin P, Zrinzo L, Brown P and Litvak V 2016 The Parkinsonian subthalamic network: measures of power, linear, and non-linear synchronization and their relationship to L-DOPA treatment and OFF state motor severity *Front. Hum. Neurosci.* **10** 517
[40] Poza J, Gómez C, Bachiller A and Hornero R 2012 Spectral and non-linear analyses of spontaneous magnetoencephalographic activity in Alzheimer's disease *J. Healthc. Eng.* **3** 299–321
[41] Yuvaraj R and Murugappan M 2016 Hemispheric asymmetry non-linear analysis of EEG during emotional responses from idiopathic Parkinson's disease patients *Cogn. Neurodyn.* **10** 225–34
[42] Yang A C, Wang S J, Lai K L, Tsai C F, Yang C H, Hwang J P, Lo M T, Huang N E, Peng C K and Fuh J L 2013 Cognitive and neuropsychiatric correlates of EEG dynamic complexity in patients with Alzheimer's disease *Prog. Neuro-Psychopharmacol. Biol. Psychiatry* **47** 52–61
[43] Syrkin-Nikolau J, Koop M M, Prieto T, Anidi C, Afzal M F, Velisar A, Blumenfeld Z, Martin T, Trager M and Bronte-Stewart H 2017 Subthalamic neural entropy is a feature of freezing of gait in freely moving people with Parkinson's disease *Neurobiol. Dis.* **108** 288–97
[44] Zorick T and Mandelkern M A 2013 Multifractal detrended fluctuation analysis of human EEG: preliminary investigation and comparison with the wavelet transform modulus maxima technique *PLoS One* **8** e68360
[45] Liu G, Zhang Y, Hu Z, Du X, Wu W, Xu C, Wang X and Li S 2017 Complexity analysis of electroencephalogram dynamics in patients with Parkinson's disease *Parkinsons Dis.* **2017** 8701061
[46] Labate D, Foresta F, La Morabito G, Palamara I and Morabito F C 2013 Entropic measures of EEG complexity in Alzheimer's disease through a multivariate multiscale approach *IEEE Sens. J.* **13** 3284–92
[47] Yi G S, Wang J, Deng B and Wei X L 2017 Complexity of resting-state EEG activity in the patients with early-stage Parkinson's disease *Cogn. Neurodyn.* **11** 147–60
[48] Vyšata O, Procházka A, Mareš J, Rusina R, Pazdera L, Vališ M and Kukal J 2014 Change in the characteristics of EEG color noise in Alzheimer's disease *Clin. EEG Neurosci.* **45** 147–51
[49] Martin S *et al* 2018 Differential contributions of subthalamic beta rhythms and 1/f broadband activity to motor symptoms in Parkinson's disease *npj Parkinsons Dis.* **4** 1–4
[50] Deng B, Liang L, Li S, Wang R, Yu H, Wang J and Wei X 2015 Complexity extraction of electroencephalograms in Alzheimer's disease with weighted-permutation entropy *Chaos* **25** 043105
[51] Mostile G, Giuliano L, Dibilio V, Luca A, Cicero C E, Sofia V, Nicoletti A and Zappia M 2019 Complexity of electrocortical activity as potential biomarker in untreated Parkinson's disease *J. Neural Transm.* **126** 167–72
[52] Smiths F M, Porcaro C, Cottone C, Cancelli A, Rossini P M and Tecchio F 2016 Electroencephalographic fractal dimension in healthy ageing and Alzheimer's disease *PLoS One* **11** e0149587
[53] Belova E M, Semenova U, Gamaleya A A, Tomskiy A A and Sedov A 2021 Voluntary movements cause beta oscillations increase and broadband slope decrease in the subthalamic nucleus of parkinsonian patients *Eur. J. Neurosci.* **53** 2205–13
[54] Coronel C, Garn H, Waser M, Deistler M, Benke T, Dal-Bianco P, Ransmayr G, Seiler S, Grossegger D and Schmidt R 2017 Quantitative EEG markers of entropy and auto mutual information in relation to MMSE scores of probable Alzheimer's disease patients *Entropy* **19** 130
[55] Pappalettera C, Miraglia F, Cotelli M, Rossini P M and Vecchio F 2022 Analysis of complexity in the EEG activity of Parkinson's disease patients by means of approximate entropy *GeroScience* **44** 1599–607
[56] Tylová L, Kukal J, Hubata-Vacek V and Vyšata O 2018 Unbiased estimation of permutation entropy in EEG analysis for Alzheimer's disease classification *Biomed. Signal Process. Control* **39** 424–30
[57] Nimmy John T, Puthankattil S D and Menon R 2018 Analysis of long range dependence in the EEG signals of Alzheimer patients *Cogn. Neurodyn.* **12** 183–99
[58] Nobukawa S, Yamanishi T, Nishimura H, Wada Y, Kikuchi M and Takahashi T 2019 Atypical temporal-scale-specific fractal changes in Alzheimer's disease EEG and their relevance to cognitive decline *Cogn. Neurodyn.* **13** 1–11
[59] Amezquita-Sanchez J P, Mammone N, Morabito F C, Marino S and Adeli H 2019 A novel methodology for automated differential diagnosis of mild cognitive impairment and the Alzheimer's disease using EEG signals *J. Neurosci. Methods* **322** 88–95
[60] Echegoyen I, López-Sanz D, Martínez J H, Maestú F and Buldú J M 2020 Permutation entropy and statistical complexity in mild cognitive impairment and Alzheimer's disease: an analysis based on frequency bands *Entropy* **22** 116
[61] Şeker M, Özbek Y, Yener G and Özerdem M S 2021 Complexity of EEG dynamics for early diagnosis of Alzheimer's disease using permutation entropy neuromarker *Comput. Methods Programs Biomed.* **206** 106116
[62] Higuchi T 1988 Approach to an irregular time series on the basis of the fractal theory *Physica* D **31** 277–83
[63] Henriques T, Ribeiro M, Teixeira A, Castro L, Antunes L and Costa-Santos C 2020 Nonlinear methods most applied to heart-rate time series: a review *Entropy* **22** 309
[64] Eke A, Hermán P, Bassingthwaighte J, Raymond G, Percival D, Cannon M, Balla I and Ikrényi C 2000 Physiological time series: distinguishing fractal noises from motions *Pflüg. Arch. Eur. J. Physiol.* **439** 403–15
[65] Delignieres D, Ramdani S, Lemoine L, Torre K, Fortes M and Ninot G 2006 Fractal analyses for 'short' time series: a re-assessment of classical methods *J. Math. Psychol.* **50** 525–44
[66] Borg F G 2005 Review of nonlinear methods and modelling (arXiv:physics/0503026) pp 1–72
[67] Coelli S, Tacchino G, Visani E, Panzica F, Franceschetti S and Bianchi A M 2019 Higher order spectral analysis of scalp EEG activity reveals non-linear behavior during rhythmic visual stimulation *J. Neural Eng.* **16** 056028

[68] Tacchino G, Coelli S, Reali P, Galli M and Bianchi A M 2020 Bicoherence interpretation in EEG requires signal to noise ratio quantification: an application to sensorimotor rhythms *IEEE Trans. Biomed. Eng.* **67** 2696–704
[69] Donoghue T *et al* 2020 Parameterizing neural power spectra into periodic and aperiodic components *Nat. Neurosci.* **23** 1655–65
[70] Perez G, Rappazzo B and Gomes C 2018 Extending the capacity of 1/f noise generation *Lecture Notes in Computer Science including subseries Lecture Notes in Artificial Intelligence and Lecture Notes in Bioinformatics* (Springer) vol 11008 LNCS pp 601–10
[71] Valencia M, Lopéz-Azcárate J, Nicoĺas M J, Alegre M and Artieda J 2012 Dopaminergic modulation of the spectral characteristics in the rat brain oscillatory activity *Chaos Solitons Fractals* **45** 619–28
[72] Pilgrim I and Taylor R P 2018 Fractal analysis of time-series data sets: methods and challenges *Fractal Analysis* ed S A Ouadfeul (Intechopen) (https://doi.org/10.5772/intechopen.81958)
[73] Higuchi T 1990 Relationship between the fractal dimension and the power law index for a time series: a numerical investigation *Physica* D **46** 254–64
[74] Ferrara R, Bianchi A, Priori A, Coelli S and Averna A 2022 Levodopa-dependent differences in the non-oscillatory activity of the subthalamic nucleus *2022 44th Annual Int. Conf. IEEE Engineering in Medicine & Biology Society (EMBC)* (*Glasgow, Scotland, United Kingdom*) (IEEE) pp 2310–3
[75] Colombo M A *et al* 2019 The spectral exponent of the resting EEG indexes the presence of consciousness during unresponsiveness induced by propofol, xenon, and ketamine *Neuroimage* **189** 631–44
[76] Yamamoto Y and Hughson R L 1993 Extracting fractal components from time series *Physica* D **68** 250–64
[77] Wen H and Liu Z 2016 Separating fractal and oscillatory components in the power spectrum of neurophysiological signal *Brain Topogr.* **29** 13–26
[78] Tayel M B and AlSaba E I 2017 Review: nonlinear techniques for analysis of heart rate variability *WSEAS Trans. Signal Process.* **13** 49–63 (available at: https://www.wseas.org/multimedia/journals/signal/2017/a145814-570.php)
[79] Kale M and Butar F 2005 Fractal analysis of time series and distribution properties of Hurst exponent *J. Math. Sci. Math. Educ.* **5** 8–19
[80] Hartmann A, Mukli P, Nagy Z, Kocsis L, Hermán P and Eke A 2013 Real-time fractal signal processing in the time domain *Physica* A **392** 89–102
[81] Kannathal N, Acharya U R, Lim C M and Sadasivan P K 2005 Characterization of EEG—a comparative study *Comput. Methods Programs Biomed.* **80** 17–23
[82] Peng C K, Buldyrev S V, Havlin S, Simons M, Stanley H E and Goldberger A L 1994 Mosaic organization of DNA nucleotides *Phys. Rev.* E **49** 1685
[83] Talkner P and Weber R O 2000 Power spectrum and detrended fluctuation analysis: application to daily temperatures *Phys. Rev.* E **62** 150–60
[84] Absil P A, Sepulchre R, Bilge A and Gérard P 1999 Nonlinear analysis of cardiac rhythm fluctuations using DFA method *Physica* A **272** 235–44
[85] Penzel T, Kantelhardt J W, Grote L, Peter J H and Bunde A 2003 Comparison of detrended fluctuation analysis and spectral analysis for heart rate variability in sleep and sleep apnea *IEEE Trans. Biomed. Eng.* **50** 1143–51
[86] Hu J, Gao J, Posner F L, Zheng Y and Tung W-W 2006 Target detection within sea clutter: a comparative study by fractal scaling analyses *Fractals* **14** 187–204
[87] Peng C K, Havlin S, Stanley H E and Goldberger A L 1998 Quantification of scaling exponents and crossover phenomena in nonstationary heartbeat time series *Chaos* **5** 82
[88] Shao Y H, Gu G F, Jiang Z Q, Zhou W X and Sornette D 2012 Comparing the performance of FA, DFA and DMA using different synthetic long-range correlated time series *Sci. Rep.* **2** 1–5
[89] Kantelhardt J W, Zschiegner S A, Koscielny-Bunde E, Havlin S, Bunde A and Stanley H E 2002 Multifractal detrended fluctuation analysis of nonstationary time series *Physica* A **316** 87–114
[90] Ferrario M, Signorini M G, Magenes G and Cerutti S 2006 Comparison of entropy-based regularity estimators: application to the fetal heart rate signal for the identification of fetal distress *IEEE Trans. Biomed. Eng.* **53** 119–25
[91] Azami H, Faes L, Escudero J, Humeau-Heurtier A and Silva L E V 2023 Entropy analysis of univariate biomedical signals: review and comparison of methods *Frontiers in Entropy across the Disciplines: Panorama of Entropy: Theory, Computation, and Applications* ed W Freeden and M Z Nashed (World Scientific) ch 9, pp 233–86
[92] Pincus S 1998 Approximate entropy (ApEn) as a complexity measure *Chaos* **5** 110
[93] Courtiol J, Perdikis D, Petkoski S, Müller V, Huys R, Sleimen-Malkoun R and Jirsa V K 2016 The multiscale entropy: guidelines for use and interpretation in brain signal analysis *J. Neurosci. Methods* **273** 175–90
[94] Bandt C and Pompe B 2002 Permutation entropy: a natural complexity measure for time series *Phys. Rev. Lett.* **88** 4
[95] Zanin M, Zunino L, Rosso O A and Papo D 2012 Permutation entropy and its main biomedical and econophysics applications: a review *Entropy* **14** 1553–77
[96] Costa M, Goldberger A L and Peng C-K 2002 Multiscale entropy analysis of complex physiologic time series *Phys. Rev. Lett.* **89** 068102
[97] Bassingthwaighte J 1988 Physiological heterogeneity: fractals link determinism and randomness in structures and functions *Physiology* **3** 5–10
[98] Caccia D C, Percival D, Cannon M J, Raymond G and Bassingthwaighte J B 1997 Analyzing exact fractal time series: evaluating dispersional analysis and rescaled range methods *Physica* A **246** 609–32
[99] Cannon M J, Percival D B, Caccia D C, Raymond G M and Bassingthwaighte J B 1997 Evaluating scaled windowed variance methods for estimating the Hurst coefficient of time series *Physica* A **241** 606–26
[100] Chen Z, Ivanov P C, Hu K and Stanley H E 2002 Effect of nonstationarities on detrended fluctuation analysis *Phys. Rev.* E **65** 041107
[101] Dehghani N, Bédard C, Cash S S, Halgren E and Destexhe A 2010 Comparative power spectral analysis of simultaneous elecroencephalographic and magnetoencephalographic recordings in humans suggests non-resistive extracellular media *J. Comput. Neurosci.* **29** 405–21
[102] Gerster M, Waterstraat G, Litvak V, Lehnertz K, Schnitzler A, Florin E, Curio G and Nikulin V 2022 Separating neural oscillations from aperiodic 1/f activity: challenges and recommendations *Neuroinformatics* **20** 991–1012
[103] Kuntzelman K, Jack Rhodes L, Harrington L N and Miskovic V 2018 A practical comparison of algorithms for the measurement of multiscale entropy in neural time series data *Brain Cogn.* **123** 126–35
[104] Theiler J, Eubank S, Longtin A, Galdrikian B and Doyne Farmer J 1992 Testing for nonlinearity in time series: the method of surrogate data *Physica* D **58** 77–94
[105] Lancaster G, Iatsenko D, Pidde A, Ticcinelli V and Stefanovska A 2018 Surrogate data for hypothesis testing of physical systems *Phys. Rep.* **748** 1–60
[106] Averna A, Marceglia S, Priori A and Foffani G 2022 Amplitude and frequency modulation of subthalamic beta oscillations jointly encode the dopaminergic state in Parkinson's disease *npj Parkinsons Dis.* **8** 131

[107] Averna A, Arlotti M, Rosa M, Chabardès S, Seigneuret E, Priori A, Moro E and Meoni S 2022 Pallidal and cortical oscillations in freely moving patients with dystonia *Neuromodulation* (https://doi.org/10.1111/ner.13503)
[108] Babiloni C *et al* 2021 Measures of resting state EEG rhythms for clinical trials in Alzheimer's disease: recommendations of an expert panel *Alzheimer's Dementia* **17** 1528–53
[109] Averna A, Marceglia S, Arlotti M, Locatelli M, Rampini P, Priori A and Bocci T 2022 Influence of inter-electrode distance on subthalamic nucleus local field potential recordings in Parkinson's disease *Clin. Neurophysiol.* **133** 29–38
[110] Abásolo D, Hornero R, Escudero J and Espino P 2008 A study on the possible usefulness of detrended fluctuation analysis of the electroencephalogram background activity in Alzheimer's disease *IEEE Trans. Biomed. Eng.* **55** 2171–9
[111] Botcharova M, Berthouze L, Brookes M J, Barnes G R and Farmer S F 2015 Resting state MEG oscillations show long-range temporal correlations of phase synchrony that break down during finger movement *Front. Physiol.* **6** 183
[112] Stam C J 2005 Nonlinear dynamical analysis of EEG and MEG: review of an emerging field *Clin. Neurophysiol.* **116** 2266–301
[113] Andres D S and Darbin O 2018 Complex dynamics in the basal ganglia: health and disease beyond the motor system *J. Neuropsychiatry Clin. Neurosci.* **30** 101–14
[114] Darbin O, Dees D, Martino A, Adams E and Naritoku D 2013 An entropy-based model for basal ganglia dysfunctions in movement disorders *Biomed. Res. Int.* **2013** 1–5
[115] Tzimourta K D, Christou V, Tzallas A T, Giannakeas N, Astrakas L G, Angelidis P, Tsalikakis D and Tsipouras M G 2021 Machine learning algorithms and statistical approaches for Alzheimer's disease analysis based on resting-state EEG recordings: a systematic review *Int. J. Neural Syst.* **31** 2130002